Power circulation via negative energy-flux wormholes in optical nanowaveguides

Sergiy Mokhov, Ramy El-Ganainy, and Demetrios N. Christodoulides

College of Optics and Photonics/CREOL, University of Central Florida, Orlando, Florida, 32816-2700, USA
demetri@creol.ucf.edu

Abstract: We show that energy circulation within a pulse is possible when it propagates in a high-contrast dielectric nanowire. This process is accomplished through electromagnetic "wormhole" regions, in which the Poynting vector associated with the guided mode is negative with respect to the direction of propagation. For demonstration purposes this mechanism is elucidated in *AlGaAs* and silicon nanowaveguides. The effect of dispersion on the power circulation is also considered.

OCIS codes: (130.2790) Guided waves; (060.5530) Pulse propagation and solitons.

References and links

1. P. N. Prasad, *Nanophotonics*, (John Wiley and Sons, New York 2004).
2. S. Kawata, M. Ohtsu and M. Irie, *Nano-Optics*, (Springer Verlag, Berlin 2002).
3. S. G. Leon-Saval, T. A. Birks, W. J. Wadsworth, P. St. J. Russell, and M. W. Mason, "Supercontinuum generation in submicron fibre waveguides," Opt. Express **12,** 2864-2869 (2004).
4. L. Tong, R. R. Gattass, J. B. Ashcom, S. He, J. Lou, M. Shen, I. Maxwell, and E. Mazur, "Subwavelength-diameter silica wires for low-loss optical wave guiding," Nature **426**, 816-819 (2003).
5. M. A. Foster, A. L. Gaeta, Q. Cao, and R. Trebino, "Soliton-effect compression of supercontinuum to few-cycle durations in photonic nanowires," Opt. Express **13,** 6848-6855 (2005).
6. L. Scaccabarozzi, X. Yu, M. L. Povinelli, S. Fan, M. M. Fejer and J. S. Harris, "Highly efficient birefringent second harmonic generation in submicron AlGaAs/Al_xO_y waveguides," CLEO 2005 Techncial Digest, paper CPDA10.
7. R. Iwanow, G. I. Stegeman, D. N. Christodoulides, R. Morandotti, D. Modotto, A. Locatelli, C. De Angelis, C. R. Stanley, M. Sorel and J. S. Aitchison, "Enhanced third order nonlinear effects in AlGaAs nano-wire waveguides," post-deadline paper PDP7, Nonlinear guided waves and their applications, OSA Topical Meeting, Dresden, Germany, Sept. 6-9, 2005.
8. R. El-Ganainy, S. Mokhov, K. G. Makris, and D. N. Christodoulides, "Solitons in dispersion-inverted *AlGaAs* nanowires," Opt. Express **14,** 2277-2282 (2006).
9. D. Hondros and P. Debye, "Elektromagnetische Wellen an dielektrischen Drähten," Ann. Physik **32**, 465-476 (1910).
10. S. A. Schelkunoff, *Electromagnetic Waves* (D. Van Nostrand Inc., New York, 1943).
11. E. Snitzer, "Cylindrical dielectric waveguide mode," J. Opt. Soc. Am. **51**, 491-498 (1961).
12. E. F. F. Gillespie, Proc. Inst. Elect. Eng. **107**c, 198-201 (1960).
13. J. D. Jackson, *Classical Electrodynamics* (Wiley, New York, 1975).
14. K. Okamoto, *Fundamentals of Optical Waveguides* (Academic Press, London 2000).
15. Y. N. Noskov, "Method for measuring properties of high relative dielectric constant materials in a cutoff waveguide cavity," IEEE Trans. Microwave Theory Tech, **MTT-48**, 329-333 (2000).
16. I. V. Shadrivov, A. A. Sukhorukov, and Y. S. Kivshar, "Guided modes in negative-refractive-index waveguides," Phys. Rev. E **67,** 0576021-0576024 (2003).
17. S. Kawata and T. Tani, "Optically driven Mie particles in an evanescent field along a channeled waveguide," Opt. Lett. **21**, 1768-1770 (1996).
18. A. Askin, "Acceleration and trapping of particles by radiation pressure," Phys. Rev. Lett. **24**, 156-159, (1970).
19. J. P. Gordon, "Radiation forces and momenta in dielectric media," Phys. Rev. A **8**, 14-21 (1973).

#68321 - $15.00 USD Received 21 February 2006; revised 4 April 2006; accepted 8 April 2006

1. Introduction

Controlling the flow of light on a nanometer scale may have important implications in both science and technology [1]. Progress in the area of nano-photonics is expected to impact communication and computing technologies as well as bio-photonics. In the last few years we have witnessed rapid advances in the fields of near-field microscopy and spectroscopy and sub-wavelength imaging [2]. The fabrication of high contrast dielectric nanowaveguides is yet another important development in this area. Because of their strong index contrast, these sub-wavelength waveguides or nanowires can exhibit considerably altered dispersion characteristics and enhanced nonlinearity [3-5]. When implemented with semiconductor materials such as *GaAs* or *AlGaAs*, these nano-waveguides show promise for efficient second harmonic generation and self-phase modulation at very low optical powers [6-8].

In the last few decades or so, the electromagnetic problem associated with wave propagation in cylindrical dielectric waveguides has been intensely investigated in a number of studies [9-11]. Given the history of this topic, at a first glance it may seem that all is known regarding the guiding behavior of these structures. An unusual effect associated with the electromagnetic properties of the fundamental HE_{11} mode in high-contrast dielectric rods was theoretically found by Gillespie in 1960 [12]. This effect, which has so far received little if any attention, arises from the fact that in such high-contrast structures there can be two regions (close to the core-cladding boundary) where the Poynting vector is negative with respect to the direction of propagation. We emphasize that in all cases (for lossless fibers), the phase velocity and group velocity vectors of the HE_{11} mode are parallel, i.e. the negative power never exceeds the positive power and thus no backward waves are associated with the presence of these regions [12]. An important facet of this intriguing effect that still remains unresolved arises when one examines the energy balance equation of the HE_{11} mode during pulse propagation, e.g., by considering [13]

$$\oiint_A \vec{S} \cdot d\vec{a} = -\frac{\partial W}{\partial t} \tag{1}$$

over a virtual volume $\mathcal{V}$ (surrounded by a surface $\mathcal{A}$) that is totally embedded in one of these regions. In Eq. (1), $\vec{S}$ is the energy flux or Poynting vector, and W is the total electromagnetic energy in the volume $\mathcal{V}$. More specifically, if a pulse first excites the front face of the virtual surface enclosing this volume (where the energy flux is negative), then how is the escaping energy balanced in this region? To address this issue we will investigate the behavior of this system in the time domain.

In this paper we show, that in high-contrast dielectric optical nanowires, power circulation is possible during pulse propagation via negative energy-flux wormholes. This phenomenon is in fact universal since it occurs in a variety of waveguide geometries as long as the waveguide index-contrast exceeds a critical value. For demonstration purposes this mechanism is examined in circular *AlGaAs* and silicon nanowaveguides. We theoretically demonstrate that under pulse conditions these wormholes are constantly exchanging energy with their surroundings and at "infinity" (with respect to the pulse center) they become strongly warped-in a way similar to that expected in negative-index waveguides. For completeness dispersion effects are also accounted in our analysis and pertinent examples are provided. Methods to detect the presence of these negative energy-flux regions or wormholes are also suggested.

2. Analysis

To demonstrate our results we consider wave propagation in a cylindrical optical nanowire of core radius a. This dielectric rod is surrounded by air/vacuum and its refractive index is taken here to be n. The vacuum wavelength of the optical wave exciting this nano-waveguide

#68321 - $15.00 USD Received 21 February 2006; revised 4 April 2006; accepted 8 April 2006

is λ_0. In this case, the electromagnetic field associated with fundamental HE_{11} mode of this cylindrical structure is given by [14]

$$\vec{E} = \vec{e}(r,\theta)\exp[i(\omega t - \beta z)] \qquad (2a)$$

$$\vec{H} = \vec{h}(r,\theta)\exp[i(\omega t - \beta z)] \qquad (2b)$$

where its propagation constant β can be obtained from the first root of the corresponding eigenvalue equation. In this study, without any loss of generality, the fields of Eq. (2) were judiciously chosen so as the transverse electric field of the of the fundamental mode is primarily *x*-polarized (HE_{11}^{x}) [14]. As usual the transverse components ($e_r, e_\theta, h_r, h_\theta$) of the hybrid HE_{11} field can be directly derived from the longitudinal vectors. Here, the longitudinal electric fields are taken to be: $e_z = AJ_1(ur/a)\cos(\theta)$, $e_z = BK_1(wr/a)\cos(\theta)$ in the core and cladding regions respectively. Similarly, the magnetic fields are given by: $h_z = CJ_1(ur/a)\sin(\theta)$ and $h_z = DK_1(wr/a)\sin(\theta)$, where *A,B,C,D, u,* and *w,* are all frequency dependent quantities [14]. The time-averaged Poynting vector can then be obtained from $\vec{S} = (1/2)\,\mathrm{Re}(\vec{E}\times\vec{H}^{*})$ which under continuous-wave (CW) conditions has only a $\hat{z}$ -component, i.e., is parallel to the direction of propagation.

As an example, Fig. 1(a) shows the distribution of the Poynting vector S_z (of the HE_{11}^{x} mode) over the entire transverse plane (core and cladding regions) of an $Al_{0.2}Ga_{0.8}As$ nanowire when its radius is $a = 170\,nm$. The $Al_{0.2}Ga_{0.8}As$ refractive index is $n = 3.25$ and the operating wavelength was assumed to be $\lambda_0 = 1.5\mu m$. Figure 1(b) clearly shows that in this case the intensity distribution in this nanowaveguide is elliptical-like (with an aspect ratio of 80 %).

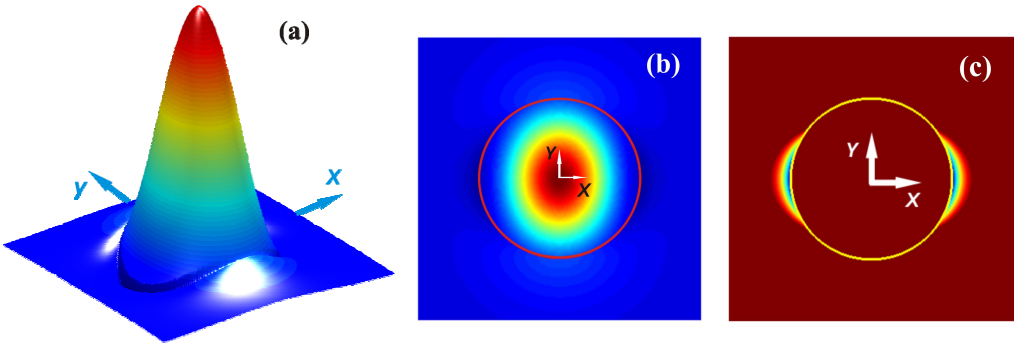

Fig.1. (a) Distribution of the HE_{11}^{x} Poynting vector S_z associated with an $Al_{0.2}Ga_{0.8}As$ nanowire of core radius $a = 170\,nm$. (b) Top view shows the ellipticity of the S_z distribution. (c) Negative S_z regions with the positive part removed for illustration purposes.

More importantly, at the core-air interface (around the *x*-axis or $\theta = 0$) there are two regions or wormholes where the energy flux density or Poynting vector becomes negative. What is quite interesting, is that, this effect results and coexists with the process of total internal

#68321 - $15.00 USD Received 21 February 2006; revised 4 April 2006; accepted 8 April 2006

reflection (TIR) which is responsible for the existence of the guided mode. These two areas have a crescent-like shape as shown in Fig. 1(c).

In general, these negative S_z features arise from the severe disruption of the electromagnetic field lines at the core-cladding interface and are only possible in high-index-contrast structures. It is worth noting that this effect does not occur for TE and TM modes since in these cases one can directly show that S_z is everywhere positive. Figure 2 shows the contour lines of $\left|S^-_{z-\max} / S^+_{z-\max}\right|$ associated with the HE_{11} mode in such a nanowire structure, as a function of index contrast and the *V*-number, where $V = (2\pi a / \lambda_0)\sqrt{n^2 - 1}$ [14].

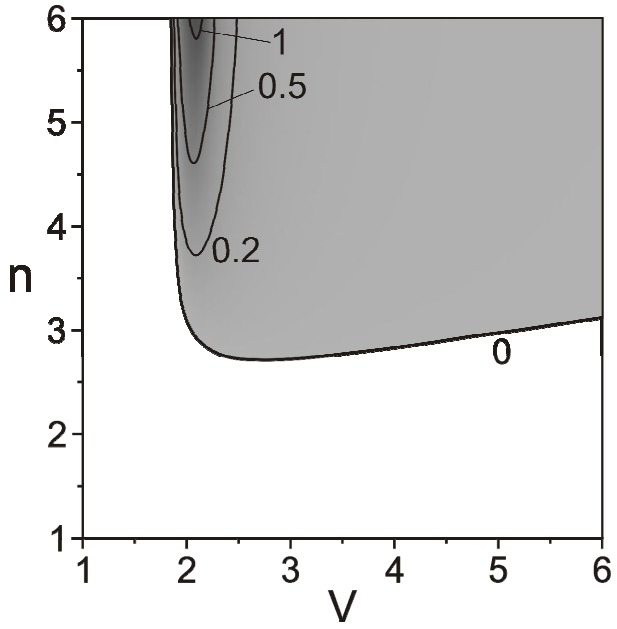

Fig. 2. Iso-contour lines $\left|S^-_{z-\max} / S^+_{z-\max}\right|$ associated with the HE_{11} mode in an air-clad nanowire, as a function of index contrast and the *V* number.

As this latter figure indicates, these wormholes start to appear only when the core index exceeds the critical value of $n \geq 2.71$. Thus these effects can take place in low-loss high-index materials such as for example *GaAs*, *AlGaAs*, or *Si*. For the $Al_{0.2}Ga_{0.8}As$ nanorod assumed here, these regions exist in the range $1.97 \leq V \leq 6.88$ (i.e. in both the single-and multi-mode regime) and its maximum $\left|S^-_{z-\max} / S^+_{z-\max}\right|$ ratio is around *10%* at *V=2.2*. Figure 2 also indicates that these effects can become considerably more pronounced at higher index contrasts. This may be more relevant in the microwave region where materials with very high refractive indices of $n \approx 8-10$ are known to exist [15].

We emphasize that these negative energy flux regions occur in a universal fashion, e.g. they are not uniquely associated with cylindrical waveguides. Figure 3 depicts the electric field distributions as well as the negative Poynting vector regions as obtained using finite element methods for three different waveguide geometries when $\lambda_0 = 1.55\mu m$. In all cases

#68321 - $15.00 USD Received 21 February 2006; revised 4 April 2006; accepted 8 April 2006

the structures are air-clad and are assumed to be made out of silicon (refractive index of Si is $n = 3.5$).

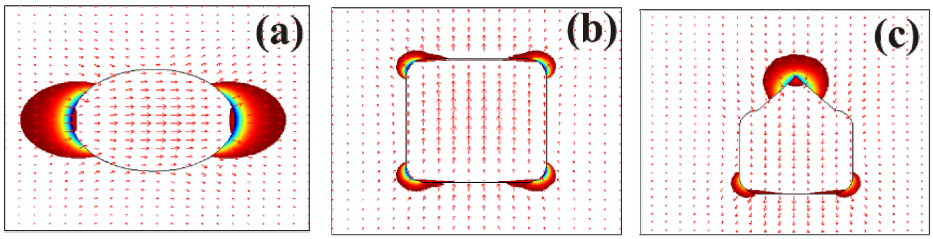

Fig. 3. Electric field and negative Poynting vector distributions in an (a) elliptical waveguide with aspect ratio $400 \times 350\, nm^2$ (b) square waveguide $350 \times 350\, nm^2$ and (c) "pyramid" waveguide of approximate dimensions $300 \times 350\, nm^2$

Note that these wormhole domains are always enhanced around edges and regions of high geometrical curvature. Thus these effects are a byproduct of high-index contrast and geometrical effects, around which the electromagnetic field lines are severely distorted.

3. Results and discussion

Even though the CW analysis indicates that such negative energy flux regions are possible in high-index optical material systems the question remains how these wormholes get established in the first place and how is their presence consistent with the energy considerations of Eq. (1). To address these issues we will examine this problem in the time domain. To do so we express both the electric and magnetic field vectors through a Fourier superposition, i.e.,

$$\begin{Bmatrix} \vec{E} \\ \vec{H} \end{Bmatrix} = \frac{e^{i(\omega_0 t - \beta_0 z)}}{2\pi} \int_{-\infty}^{\infty} d\Omega \Phi_0(\Omega)\, e^{i(\Omega T - F(\Omega) z)} \begin{Bmatrix} \vec{e}(\vec{r}_\perp, \omega_0 + \Omega) \\ \vec{h}(\vec{r}_\perp, \omega_0 + \Omega) \end{Bmatrix} \quad (3)$$

where ω_0 is the carrier angular frequency of the wavepacket and β_0 is the corresponding propagation constant of the HE_{11} mode. $T = t - z/\upsilon_g$ is a time coordinate frame moving at the group velocity υ_g of the pulse, $\Phi_0(\Omega)$ is the pulse envelope frequency spectrum, Ω is a frequency deviation from ω_0, and the dispersion function is defined as $F(\Omega) = \beta(\omega_0 + \Omega) - \beta_0 - (\Omega/\upsilon_g)$. By employing a first-order Taylor series expansion of the vector fields around ω_0, i.e., $\vec{e}(\vec{r}_\perp, \omega_0 + \Omega) = \vec{e}_0(\vec{r}_\perp) + \vec{e}_1(\vec{r}_\perp)\Omega$ where $\vec{e}_1(\vec{r}_\perp) = d\vec{e}/d\omega$ evaluated at ω_0, and similarly for the magnetic field $\vec{h}$, Eq. (3) takes the form

$$\begin{bmatrix} \vec{E} \\ \vec{H} \end{bmatrix} = \begin{bmatrix} \vec{e}_0 & -i\vec{e}_1 \\ \vec{h}_0 & -i\vec{h}_1 \end{bmatrix} \begin{bmatrix} \phi \\ \partial\phi/\partial T \end{bmatrix} \exp[i(\omega_0 t - \beta_0 z)] \quad (4)\ .$$

In Eq. (4), $\phi(z,T)$ represents the envelope of the pulse which is given by $\phi(z,T) = (1/2\pi)\int d\Omega \Phi_0(\Omega) \exp[i(\Omega T - zF(\Omega))]$. In addition, one can formally show that even under dynamic conditions the average power flow density is still given

#68321 - $15.00 USD
Received 21 February 2006; revised 4 April 2006; accepted 8 April 2006

by $\vec{S} = (1/2)\,\mathrm{Re}(\vec{E} \times \vec{H}^{*})$. This is true because, under typical pulsed conditions, the time-averaged part $(1/2)\,\mathrm{Re}(\vec{E} \times \vec{H})$ of the Poynting vector is zero as the spectral functions $\Phi_0(\omega - \omega_0)$ and $\Phi_0(-\omega - \omega_0)$ have no overlap. In this case,

$$\vec{S} = \frac{1}{2}\mathrm{Re}\left\{ A^2(\vec{e}_0 \times \vec{h}_0^{*}) + A^2 \frac{\partial \psi}{\partial T}\left(\vec{e}_1 \times \vec{h}_0^{*} + \vec{e}_0 \times \vec{h}_1^{*}\right) + \frac{i}{2}\frac{\partial A^2}{\partial T}\left(\vec{e}_0 \times \vec{h}_1^{*} - \vec{e}_1 \times \vec{h}_0^{*}\right)\right\}, \qquad (5)$$

where in Eq. (5) the envelope was expressed in polar form, e.g. $\phi = A\exp(i\psi)$. Let us now analyze this latter result. The first term in the bracket corresponds to a modulated $\hat{z}$ power flow (CW-like part). The second term in Eq. (5) describes an energy redistribution among spectral frequency components (different frequencies see a different HE_{11} distribution). From the fact that $\mathrm{Re}\left\{\vec{e}(\omega_0 + \Omega) \times \vec{h}^{*}(\omega_0 + \Omega)\right\} \times \hat{z} = 0$, one can then deduce that the energy redistribution associated with the $\mathrm{Re}\left(\vec{e}_1 \times \vec{h}_0^{*} + \vec{e}_0 \times \vec{h}_1^{*}\right)$ term occurs again only in the $\hat{z}$ direction. The last term on the other hand gives the *transverse* Poynting vector and is in fact responsible for establishing the wormhole regions. It is important to note that since $\int dT (A^2)_T = 0$ (for a finite energy pulse), the time-integrated Poynting vector $\int dT\, \vec{S}$ of Eq. (5) exhibits only a $\hat{z}$ component, in agreement with Parseval's energy theorem. If we assume that initially the envelope is Gaussian, that is $\phi(z = 0, T) = E_0 \exp(-T^2/\tau_0^2)$ and by considering only second-order dispersion effects ($F(\Omega) = \beta_0^{''}\Omega^2/2$), then the evolution of the envelope in Eq. (5) can be analytically determined. In this latter case, $\vec{S}$ is given by

$$\vec{S} = \frac{|E_0|^2}{2\sqrt{1 + (z/z_d)^2}} \exp\left(-\frac{2\tau^2}{1 + (z/z_d)^2}\right) \cdot \qquad (6)$$

$$\mathrm{Re}\left\{\left(\vec{e}_0 \times \vec{h}_0^{*}\right) + \frac{2(\tau/\tau_0)(z/z_d)}{1 + (z/z_d)^2}\left(\vec{e}_1 \times \vec{h}_0^{*} + \vec{e}_0 \times \vec{h}_1^{*}\right) - \frac{2i(\tau/\tau_0)}{1 + (z/z_d)^2}\left(\vec{e}_0 \times \vec{h}_1^{*} - \vec{e}_1 \times \vec{h}_0^{*}\right)\right\}$$

where $\tau = T/\tau_0$ is a normalized time coordinate and $z_d = \tau_0^2/\left(2\beta_0^{''}\right)$ is a dispersion length. As an example we consider the propagation of a Gaussian pulse in an $Al_{0.2}Ga_{0.8}As$ nanowire at $\lambda_0 = 1.5\mu m$, when the core radius is $a = 170\,nm$, the nanowire dispersion is $\beta_0^{''} = 4.48\,ps^2/m$, and the pulsewidth is $\tau_0 = 500\,fs$. Figure 4(a) depicts the transverse Poynting vector associated with this case, as obtained from Eq. (6), at $T/\tau_0 = -1$ (at the leading edge of the pulse) after a propagation distance of one dispersion length, $L = |z_d|$. As Fig. 4(a) clearly indicates, the two negative energy flux wormholes are constantly fed with energy from the sides, from both the core and cladding regions. This energy sinkhole effect is better shown in Fig. 4(b), where the wormhole has been expanded for illustration purposes. On the other hand, at the trailing part of the pulse ($T/\tau_0 > 0$), the situation is reversed, i.e., the wormholes release their energy to the forward S_z components, i.e., they act as sources.

#68321 - $15.00 USD Received 21 February 2006; revised 4 April 2006; accepted 8 April 2006

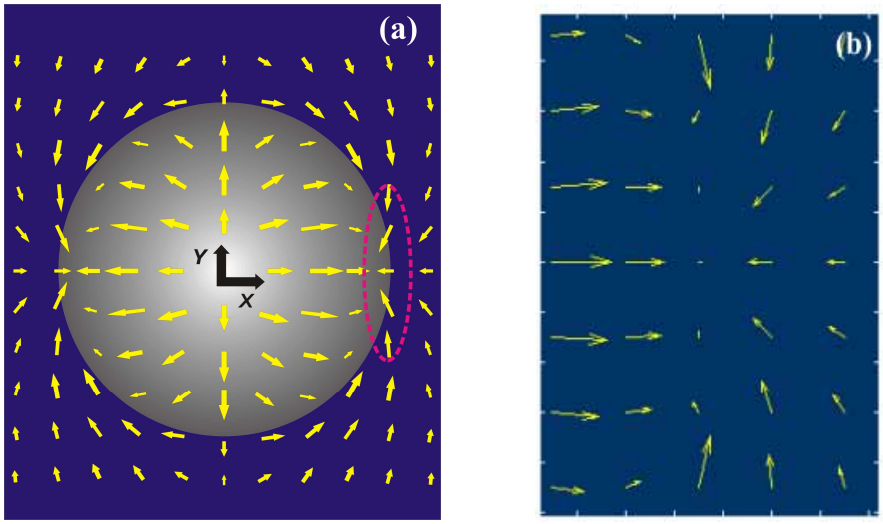

Fig. 4. (a) Transverse Poynting vector distribution at the leading edge of a pulse (b) An expanded view of the power-flow density around the wormhole area.

Even more importantly, at a certain time-distance (ahead or behind the pulse center) where the power tends to diminish, these wormholes become strongly warped. This warping effect of the power-flow density is schematically illustrated in Fig. 5, in the $x-T$ plane.

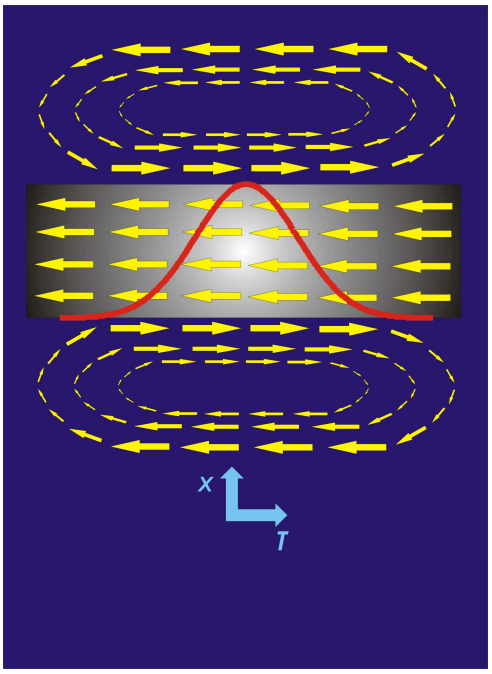

Fig. 5. Schematic demonstration of the space-time Poynting vector field (in *T* and *x*). Power circulation within the pulse (traveling from right to left) is evident.

#68321 - $15.00 USD Received 21 February 2006; revised 4 April 2006; accepted 8 April 2006

Our results shed light on how such an energy balance is accomplished around these negative S_z zones. More specifically, at the front of the pulse, these wormholes are fed from the positive S_z regions (from core and cladding) whereas at the back of the pulse this energy is returned. Even under CW conditions, this same reasoning is still applicable if one considers the time history (pulse-fronts) of this field at $T \to \pm\infty$. It is important to note that the mechanism responsible for setting up the power circulation in these nanowires is fundamentally different from the one involved in similar effects in negative-index (metamaterial) waveguides [16]. As we pointed out before these effects arise because of high-index contrast and geometrical effects.

One possible avenue to detect the presence of these wormholes is to observe the effect of negative S_z on nanoparticles given that these regions primarily exist in the air/vacuum cladding. Since the longitudinal radiation force component is parallel to the S_z vector [17-19], then particles located within the wormholes are expected to move towards the source. This is in contrast to what happens in similar configurations using low contrast waveguide structures (particles are repelled away from the source). From the previous discussion the direction of the force is expected to be polarization dependent. Other methods to detect this "negative wind" from dielectric waveguides are also currently considered.

4. Conclusion

In conclusion we have shown that that power circulation is possible during pulse propagation in high-contrast optical nanowires. This process is accomplished via negative energy-flux wormholes that are constantly exchanging energy with their surroundings. Our results explain how these zones are formed and provide a detailed account as to their energy balance. The implications of our results on other aspects concerning wave propagation in optical nanowires are currently investigated.

Acknowledgments

The authors acknowledge useful discussions with Drs. G. I. Stegeman and B. Zeldovich. This work was supported in part by the US National Science Foundation.

#68321 - $15.00 USD Received 21 February 2006; revised 4 April 2006; accepted 8 April 2006